Mathematical Biosciences and Engineering

http://www.aimspress.com/journal/mbe

MBE, 20(9): 16015–16032.
DOI: 10.3934/mbe.2023714
Received: 10 May 2023
Revised: 24 June 2023
Accepted: 10 July 2023
Published: 04 August 2023

Research article

An immuno-epidemiological model linking between-host and within-host dynamics of cholera

Beryl Musundi[1,2,*]

[1] Faculty of Mathematics, Technische Universität München, 85748 Garching, Germany
[2] Department of Mathematics, Moi University, 3900-30100 Eldoret, Kenya

* **Correspondence:** Email: beryl.musundi@tum.de.

Abstract: Cholera, a severe gastrointestinal infection caused by the bacterium *Vibrio cholerae*, remains a major threat to public health, with a yearly estimated global burden of 2.9 million cases. Although most existing models for the disease focus on its population dynamics, the disease evolves from within-host processes to the population, making it imperative to link the multiple scales of the disease to gain better perspectives on its spread and control. In this study, we propose an immuno-epidemiological model that links the between-host and within-host dynamics of cholera. The immunological (within-host) model depicts the interaction of the cholera pathogen with the adaptive immune response. We distinguish pathogen dynamics from immune response dynamics by assigning different time scales. Through a time-scale analysis, we characterise a single infected person by their immune response. Contrary to other within-host models, this modelling approach allows for recovery through pathogen clearance after a finite time. Then, we scale up the dynamics of the infected person to construct an epidemic model, where the infected population is structured by individual immunological dynamics. We derive the basic reproduction number ($\mathcal{R}_0$) and analyse the stability of the equilibrium points. At the disease-free equilibrium, the disease will either be eradicated if $\mathcal{R}_0 < 1$ or otherwise persists. A unique endemic equilibrium exists when $\mathcal{R}_0 > 1$ and is locally asymptotically stable without a loss of immunity.

Keywords: cholera; within-host dynamics; between-host dynamics; immuno-epidemiological; stability analysis

1. Introduction

Infectious diseases remain a major cause of human mortality and morbidity, despite advances in medicine [1]. A holistic understanding of the transmission dynamics of these diseases is necessary for the development of better approaches aimed at reducing their transmission [2]. Two scales of interactions can be attributed to host-pathogen interactions: the epidemiological (between-host) scale that is linked to disease transmission in the population and the immunological (within-host) scale that

relates to viral-cell interaction at the individual host level [3, 4]. The two scales have been modelled independently in many instances, as seen in [5, 6]. However, models with multiple scales that bridge between-host and within-host processes provide novel perspectives on host-parasite interactions. Such models, called immuno-epidemiological models, have gained interest in recent times [7]. These models incorporate both the immunological and epidemiological processes, allowing for a better understanding of the complex interactions between pathogens and hosts. Multi-scale (immuno-epidemilogical) models provide benefits such as explaining the role of within-host processes in pathogen evolution and predicting epidemiological quantities such as reproduction numbers and disease prevalence. Aside from the between and within-host processes, the linkage mechanism is a critical aspect in connecting the two processes [7, 8]. Examples of linkage mechanisms include linkage through nesting principles and the formulation of immunologically inspired between-host models [9].

The present paper focuses on an immuno-epidemiological model for cholera, which is an acute gastrointestinal disease caused by the bacterium *Vibrio cholerae*. The disease affects millions of people globally, mainly in countries that lack access to safe drinking water and proper sanitation infrastructure. The global burden is estimated at 2.9 million cases and 95,000 deaths annually [10]. Cholera is transmitted directly through the fecal-oral route and indirectly from the environment through ingestion of contaminated food and water [11]. The transmission dynamics of the disease spans multiple scales and are largely dependent on the diverse interactions between the environment, the human host, and the pathogen [11]. When bacteria are ingested, through either route of transmission, they must survive the stomach's gastric acid. Then, they penetrate the mucus lining of the epithelial cells, colonize them, and secrete a Cholera toxin (CT) that causes cholera symptoms [12]. These symptoms include watery diarrhoea and vomiting. Infected persons are either symptomatic or asymptomatic and can shed bacteria back into the environment through their stool. The passage of bacteria through the gut transforms it into a hyperinfectious state, with studies indicating that freshly shed vibrios are more infectious than the bacteria in the environment (environmental vibrios). They are also responsible for the explosive nature of the disease [11]. Therefore, the transmission dynamics evolve from complex within-host processes to between-host transmission with interactions from the cholera pathogen in the environment, making it essential to incorporate multiple scales in disease model development.

The majority of cholera models center on its epidemic spread [5, 11, 13–15]. A within-host model based on the bacterial-viral interaction of the disease [6] is among the few attempts at modelling the disease at the within-host scale. Recent attempts have also been made to develop and analyse multi-scale cholera models. Wang and Wang [16] formulated a multi-scale model that linked the between-host and within-host dynamics of cholera through human vibrio concentration. The within-host model depicts the evolution of highly infectious human vibrios in the body, whereas the between-host model is a Susceptible-Infected-Recovered (SIR) system that includes a compartment for environmental bacteria. The highly infectious human vibrios contribute to environmental bacterial growth and disease transmission among humans, providing a linkage between the two scales. Within-host dynamics occur at a faster time scale (hours) than between-host dynamics (months), allowing for a fast-slow analysis and a detailed study of the dynamics at each scale. The within-host system however takes a single ordinary differential equation form. Ratchford and Wang [17] extended the model through the inclusion of a compartment for viruses and immune responses in the within-host model. This allowed for a more detailed examination of the disease dynamics within a host. The complete model was decoupled into three subsystems, with a time-scale separation allowing for simplified analysis. The results indicate that the basic reproduction number depends on both the direct and indirect

transmission pathways of the disease.

Similarly, in this paper, we aim to extend the knowledge of multi-scale cholera modelling by formulating an immuno-epidemiological model that links the within-host and between-host dynamics of cholera. Unlike the previous papers, we structure the between-host model using immunological variables. To that end, we first derive a within-host model depicting the interaction of the cholera pathogen and the adaptive immune response. We distinguish pathogen dynamics from immune response dynamics by assigning different time scales, with pathogen dynamics being faster than the immune response. This is also more mathematically convenient, as it allows for the use of time-scale seperation methods in the analysis of the within-host model. The results from the analysis allow us to characterize a single infected individual by their immune response state. Then, we scale up the dynamics of the single infected person to construct an epidemic model where the infected population is structured by individual immunological dynamics. Lastly, we analyse the physiologically structured epidemic model to determine the long-term behavior of solutions.

The remainder of this paper is organised as follows. In Section 2, we formulate the within-host model and carry out a time-scale analysis of the fast and slow subsystems. In Section 3, we formulate the between-host model, compute the equilibrium points, derive the expression for the reproduction number and analyse the local stability of the steady states. Finally, we discuss the results and conclude the paper in Section 4.

2. Within-host model

We aim to construct a model that outlines the interaction of cholera pathogens with immune responses within an individual. We follow a similar approach described in [7]. In this case, we consider the growth of the pathogen to be influenced by Allee effects. Allee effects depict the co-relation between the population size and the fitness of a species [18, 19]. Populations exhibiting this effect show reduced growth at low pathogen densities. The effects are classified as strong if they result in a critical population density and weak if they don't result in a critical density [18]. We consider the case of strong Allee effects and assume that the Vibrio pathogens grow above a critical density for infection to occur. This turns out to be biologically relevant since microbial populations with quorum sensing mechanisms, such as *Vibrio cholerae* bacteria, have been shown to exhibit Allee effects [20, 21]. Subsequently, when ingested from the environment, cholera bacteria must first penetrate the mucus lining of the intestinal epithelial cells and escape the innate immunity defenses to be able to proliferate [12, 22]. At low densities, the innate immune responses can fight off the bacteria, and therefore a high infectious dose of 10^8–10^{11} cells is required for the bacteria to colonize the small intestines and cause infection [23].

With that in mind, we formulate the within-host model where we describe the interaction of the pathogen with the adaptive immune response. We denote the quantity of pathogen in an individual resulting from the ingestion of *Vibrio cholerae* bacteria by a pathogen load P (cells/ml). Pathogen growth in the body is subject to Allee effects, which are represented by a cubic growth term. The presence of the pathogen in the body stimulates immune response cells (B-Cells) that fight the pathogen. We denote this adaptive immune response by the variable W (cells/ml).

Therefore, the within-host model reads as follows:

$$\begin{aligned} \frac{dP}{dt} &= \alpha P\left(1-\frac{P}{K}\right)\Big(P-\beta\Big) - \gamma P - \delta PW \\ \frac{dW}{dt} &= \epsilon\Big(\kappa P - cW\Big), \end{aligned} \tag{2.1}$$

where α is the intrinsic growth rate, β is the critical density (Allee threshold) below which the pathogen has reduced growth rates and K is the carrying capacity. The pathogen is removed through natural death at rate γ and through clearance by the immune response at rate δ. The immune response is activated in the presence of the pathogen at rate κ and self-deactivated at rate c. Adaptive immune responses are known to be slower to respond to pathogens than innate responses [24]. As such, we consider that the pathogen grows at a much faster rate than the immune response. Therefore, we explicitly distinguish pathogen dynamics from immune responses by prescribing different time scales. The parameter $\epsilon \ll 1$ is the time scale parameter that represents the slow time scale of the immune response. This turns out to be mathematically convenient for analysis. Time-scale separation methods have become common in the study of biological systems after their advancement through the work of FitzHugh and Nagumo [25, 26]. The analysis of the resulting system involves splitting the full system into smaller subsystems (fast and slow systems). For an introduction to the approach, we refer the reader to [3, 25–27]. Next, we use the time-scale approach to analyse the within-host model.

2.1. Time-scale analysis

Pathogen dynamics and the dynamics of the immune response occur on separate time scales. The pathogen load is considered to grow on a fast time scale, while the immune response grows on a slow time scale. We split the system (2.1) into fast and slow systems and analyse the dynamics of each system. From the fast system, we expect to find the line of stationary points (slow manifold) along which the slow system moves. The slow system will be the reduced problem from which generalizations about the long-term behaviour of the full system can be made. That is, we can find the approximate solution for the full system.

2.1.1. Fast system

We consider the pathogen load P to be the fast variable. On the fast time scale, the immune response W does not change. Therefore, we let W be constant and only consider the change in the pathogen load. For $\epsilon \to 0$, the fast system is given by the following:

$$\begin{aligned} \frac{dW}{dt} &= 0 \\ \frac{dP}{dt} &= \alpha P\left(1 - \frac{P}{K}\right)(P - \beta) - \gamma P - \delta P W. \end{aligned} \tag{2.2}$$

The trajectories of the fast system tend to be stationary points, as seen in the next proposition.

Proposition 2.1. *System (2.2) exhibits three branches of stationary states: one trivial uninfected branch* $(W, 0)$ *and two infected branches* $(W, P_{1,2})$ *with*

$$P_{1,2} = \frac{\alpha(\beta + K) \pm \sqrt{\alpha^2(\beta + K)^2 - 4\alpha K(\alpha\beta + \gamma + \delta W)}}{2\alpha}$$

which exist for $\alpha \geq \alpha_0 = \frac{4K(\gamma + \delta W)}{(\beta - K)^2}$.

The trivial and the upper infected branches are locally asymptotically stable, while the lower infected branch is unstable. At $\alpha = \alpha_0$*, a saddle-node bifurcation takes place.*

Note that we can represent the infected branches by $(W, P) = (\phi(P), P)$ with

$$\phi(P) = \frac{\alpha}{\delta}\left(1 - \frac{P}{K}\right)(P - \beta) - \frac{\gamma}{\delta}$$

as can be seen in the proof below.

Proof. As $\frac{dW}{dt} = 0, W$ is fixed. We only consider $\frac{dP}{dt}$ for a given $W \in \mathbb{R}_+$. To find the equilibrium points, we set the right-hand side of system (2.2) to zero:

$$0 = \Big(\alpha\,(1 - \frac{P}{K})(P - \beta) - \gamma - \delta W\Big)P. \tag{2.3}$$

Equation (2.3) defines the slow manifold of the system, which can also be expressed as the following:

$$\{P = 0\} \cup \{\phi(P) = W\}, \tag{2.4}$$

where $\phi(P) = \frac{\alpha}{\delta}\,(1 - \frac{P}{K})(P - \beta) - \frac{\gamma}{\delta}\}$. We let

$$f(P, W) = \alpha P\,(1 - \frac{P}{K})(P - \beta) - \gamma P - \delta PW$$

such that $\frac{dP}{dt} = f(P, W)$. Then, the line $P = 0$ is the infection-free equilibrium, and for any point $P_0 = (0, W)$ on the line,

$$\frac{\partial}{\partial P} f(P_0) = -(\alpha\beta + \gamma + \delta W) < 0, \tag{2.5}$$

thus, the infection-free equilibrium point is locally asymptotically stable. The curve $\phi(P)$ yields the non-trivial equilibrium. We can rewrite it as the following:

$$\begin{aligned} 0 &= \alpha P^2 - \alpha(\beta + K)P + (\gamma + \delta W + \alpha\beta)K \\ P_{1,2} &= \frac{\alpha(\beta + K) \pm \sqrt{\alpha^2(\beta + K)^2 - 4\alpha K(\alpha\beta + \gamma + \delta W)}}{2\alpha}. \end{aligned} \tag{2.6}$$

Then, it follows that two positive non-trivial stationary points $P_{1,2}$ exist whenever

$$\alpha \geq \alpha_0 = \frac{4K(\gamma + \delta W)}{(\beta - K)^2}.$$

A saddle-node bifurcation (fixed point created and destroyed) occurs at the point $\alpha = \alpha_0$. Moreover, the stability of the non-trivial equilibrium point is a direct consequence of $f(P)$ being a polynomial of the third order. Therefore, the upper branch of $\phi(P)$ is stable while the lower branch is unstable.

2.1.2. Slow system

We consider the immune response W to be the slow variable. Denoting the slow time scale as τ, (i.e., $\tau = \epsilon t$), we express the slow system dynamics as the following:

$$\begin{aligned} \epsilon\frac{dP}{d\tau} &= \alpha P\,(1 - \frac{P}{K})(P - \beta) - \gamma P - \delta PW \\ \frac{dW}{d\tau} &= \kappa P - cW. \end{aligned}$$

On the singular limit, the system reduces to the following:

$$0 = \alpha\,P(1 - \frac{P}{K})(P - \beta) - \gamma P - \delta PW \tag{2.7}$$

$$\frac{dW}{dt} = \kappa P - cW. \tag{2.8}$$

Notice that Eq (2.7) is the slow manifold of the fast system (2.2). We sketch the slow manifold in Figure 1a below. We take the upper branch of the slow manifold ($\phi(P)$) to represent the fate of an infected individual (infected branch) and the lower branch ($P = 0$) to represent the recovery process (recovered branch). On the fast scale (Figure 1b), the fast dynamics drive the trajectories towards the recovered branch and the upper segment of the infected branch since both are stable. Then, we use Eq (2.8) to investigate what happens to the stable branches of the slow manifold, where P is now given in terms of W. The line $\dot{W} = \kappa P - cW = 0$ (from Eq (2.8)) intimates the direction of movement on the manifold, that is, if movement is either to the left or right of the manifold.

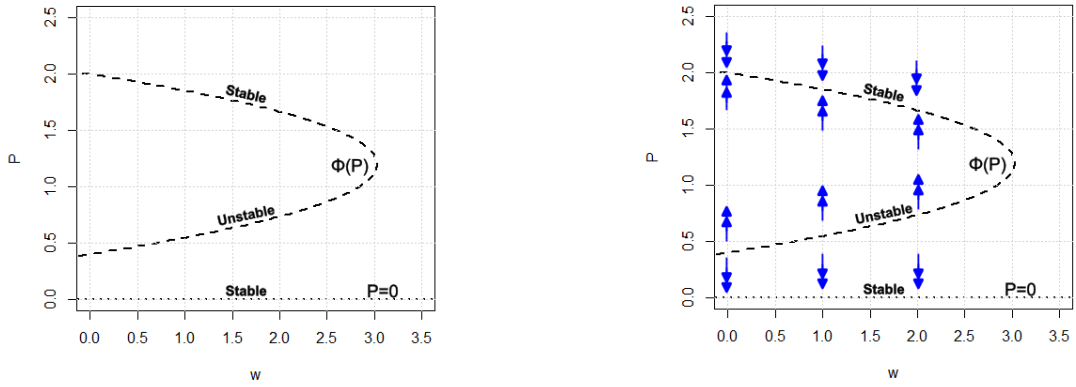

(a) Slow manifold

(b) Fast dynamics

Figure 1. The slow manifold and the trajectories on the fast scale. The blue arrows represent the direction of movement of the trajectories on the fast scale.

On the slow scale, solutions below the line $\dot{W} = 0$, that is, on the recovered branch, move to the left towards the origin $(P, W) = (0, 0)$, which is a locally stable fixed point, while solutions above the line move to the right (Figure 2a).

We observe some minimum pathogen threshold dynamics in Figure 2a (i.e., the pathogen has a significant amount (around 2.0) at the start of the immune response). Note that we only consider the case where $\frac{c}{\kappa}$ is small enough that $\{\kappa P = cW\} \cap \{W = \phi(P)\} = \emptyset$, that is, there is no chronic infection stationary state.

Since the slow system can be used to generalize the long-term behaviour of the full within-host system (2.1), we make conclusions about the infection process by shifting our attention to the infected branch of the slow manifold ($\phi(P)$). We discuss this below in more detail. The infection starts once the pathogen threshold is surpassed. As shown in Figure 2b, solutions on the upper stable branch of the infected manifold are driven to the right until the tip of the manifold is reached. At this point, due to the lower branch of $\phi(P)$ being unstable, movement along the manifold is inhibited, and the fast dynamics force a jump into the recovered branch ($P = 0$) of the manifold which is also stable. The immune response is heightened during the infection process. Consequently, the state of the immune response at the start of infection is different from that at the point of recovery. We note the state of the immune response at different points. We let the immune response at the start of infection be $W = 0 = W_0^*$ and at the point of recovery (where the jump to the recovered branch takes place) be $W = W_0$. It then follows

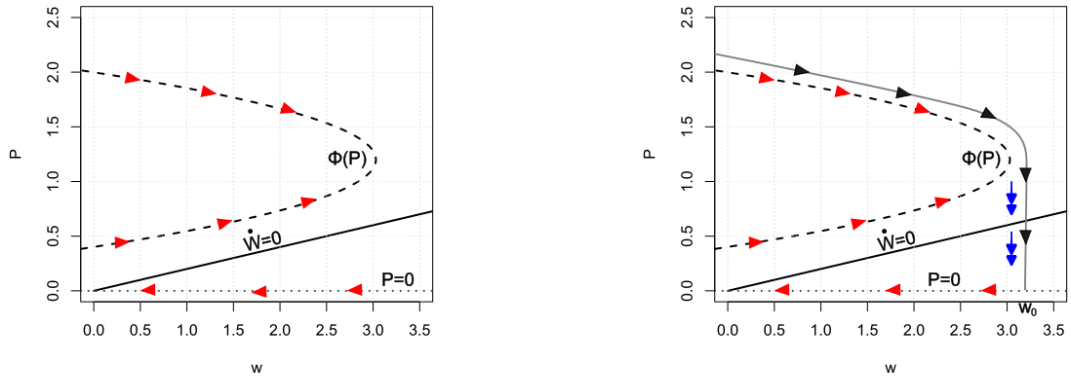

(a) Slow system

(b) Fast-slow system

Figure 2. Trajectories on the slow scale and the full system. The blue arrows represent movement on the fast scale, the red arrows represent movement on the slow scale and the black arrows represent the movement of the trajectories in the full system.

that we can describe the dynamics of the immune response by the following;

$$\frac{dW}{dt} = \kappa\phi^{-1}(W) - cW = g(W), \tag{2.9}$$

where the function $\phi^{-1}(W)$ comes from $W = \phi(P)$ being a stationary solution (see Eq (2.4)). We take note that the dynamics of P can be recovered from the equation and describe the function $g(W)$ to be the growth rate of the immune response. That is,

$$g(W) = \kappa\phi^{-1}(W) - cW, \quad \dot{W} = g(W), \quad W \in [0, W_0]. \tag{2.10}$$

Additionally, we have $g(W) > 0$ for all $W \in [0, W_0]$ such that the immune response grows with time. We can now describe the dynamics within a single infected person in terms of the immune response. We note that at the beginning of an infection, the state of the immune response is denoted by W_0^* ($W_0^* = 0$), and at the point of recovery, it is denoted by W_0. Notice that we only focus on immunity changes along the infected branch. For the recovery branch $P = 0$, we simply note that the response declines exponentially. For simplicity, we refer to the state of the immune response as immune status.

Remark 2.2. *We have expressed the within-host model in terms of the immune changes, as seen in Eq (2.9). Therefore, each infected individual's dynamics follow this expression. Then, we scale the individual dynamics to structure the infected population. The immune response levels in the infected population range from $W = 0$, which is the minimum level that corresponds to the beginning of the infection, to $W = W_0$, which is the maximal level that marks the end of the infection (recovery point). Then, the total infected population is the sum of all individuals with different immune response levels.*

In the next section, we scale up the within-host dynamics to formulate the between-host model.

3. Between-host model

We derive the between-host model based on the immunological properties. It turns out that a structured epidemiological model naturally emerges from within-host dynamics. The use of physiologically

structured models to study populations has been advanced by the work of [28–31]. The structuring variables include age, size, immunity, and many others. In [32, 33] immunological variables are used to structure the population. Similarly, using the immune status, we formulate the between-host model. We subdivide the human population into three compartments that represent the number of susceptible individuals S, the number of infected individuals I, and the number of immune/recovered individuals V. Additionally, we include a compartment B to represent the concentration of *Vibrio cholerae* bacteria in the contaminated water supply. Susceptible individuals are recruited into the population at rate r and removed by natural death at rate μ_1. Individuals in the infected compartment are structured by their within-host immune status, as described in Section 2.1 above, such that the total infected population:

$$I(t) = \int_0^{W_0} i(t, W)\, dW,$$

where $i(t, W)$ is the density of infected individuals with immune status W. Transmission of the disease occurs through the consumption of contaminated food and water (indirect) and human-human contact (direct) [11]. As such, we take both transmission pathways into account by assigning a rate β_h as the direct transmission rate and β_e as the indirect transmission rate. We consider the infectivity of an infectious person to be dependent on the within-host pathogen load P. Given that the pathogen load is influenced by the state of the immune response along the way addressed in Section 2.1, we take $P = P(W)$. Therefore, the force of infection in directly transmitted cases is proportional to the pathogen load. Natural death removes infected individuals at a rate of $\mu_2(W)$, and recovery occurs when immunity builds to the point where the pathogens are eliminated from the body. The recovery rate at that point is given as $g(W_0)$. Immunity wanes at a rate of ρ, such that an immune individual becomes susceptible once again. Immune individuals are further removed through natural death at rate μ_3. The bacteria in the environment grow through shedding by infected individuals. Shedding, which occurs at rate $\xi(W)$, is proportional to the pathogen load in an infected individual. The bacteria decay at rate σ. All in all, the between-host model reads as follows:

$$\begin{aligned}
\frac{dS(t)}{dt} &= r - \mu_1 S(t) - S(t) \int_0^{W_0} \beta_h P(W)\, i(t, W)\, dW - \beta_e S(t) B(t) \\
&\quad + \rho V(t) \\
\partial_t i(t, W) + \partial_W (g(W) i(t, W)) &= -\mu_2(W)\, i(t, W) \\
g(0) i(t, 0) &= S(t) \int_0^{W_0} \beta_h P(W) i(t, W)\, dW + \beta_e S(t) B(t) \\
\frac{dV(t)}{dt} &= g(W_0) i(t, W_0) - \rho V(t) - \mu_3 V(t) \\
\frac{dB(t)}{dt} &= \int_0^{W_0} \xi(W) P(W)\, i(t, W)\, dW - \sigma B(t),
\end{aligned} \tag{3.1}$$

with initial conditions $S(0) = S_0, \quad V(0) = V_0, \quad B(0) = B_0, \quad i(0, W) = \Phi(W)$, and $g(W)$ is defined in Eq (2.10).

3.1. Existence and uniqueness of solutions

The standard approach for showing the existence and uniqueness of solutions for structured models such as system (3.1) is to first transform the PDE problem into a renewal equation by integration along the characteristic curves. Similarly, we integrate the initial and boundary value problem for i along the characteristics.

Proposition 3.1. *Assume $i(t,0)$ is given, the solution of the PDE in the system (3.1) with the initial and boundary conditions is given by*

$$i(t,W) = \begin{cases} \Phi(G^{-1}(G(W)-t))\,\frac{g(G^{-1}(G(W)-t))}{g(W)}\,e^{-\int_{G^{-1}(G(W)-t)}^{W}\frac{\mu_2(\tau)}{g(\tau)}d\tau} & W \geq 0 \\ H(t-G(W))\frac{1}{g(W)}\,e^{-\int_0^W \frac{\mu_2(\tau)}{g(\tau)}d\tau} & W < 0, \end{cases}$$

with $G(W) = \int \frac{dW}{g(W)}$ and $H(t) = g(0)i(t,0)$.

Now that we have the solution of $i(t,W)$ along the characteristics, the proof of existence and uniqueness can be evaluated similarly to [34–37].

3.2. Basic reproduction number and stability of the DFE

The basic reproduction number $\mathcal{R}_0$ is defined as the expected number of secondary infections produced when a single infected person is introduced into a purely susceptible population [38]. It is clear that a trivial disease-free equilibrium (DFE) for system (3.1) given by $\mathcal{E}_0 = (S_0^*, 0, 0, 0)$ where $S_0^* = \frac{r}{\mu_1}$ always exists. In this section, we investigate the local stability of the DFE by linearizing the system (3.1) around the disease-free equilibrium. In so doing, we derive the threshold condition for the spread of the disease that we consider to be the basic reproduction number. We note that we consider a stability analysis with respect to the point spectrum. This is generally a sufficient condition for a linear stability analysis, that is, we presume that the point spectrum is contained in the left half plane $\mathrm{Re}(z) < 0$ (see [39, Section 3.1.2]). To complete the proof of local stability we will need to show the connection between the roots of the characteristic equation and the stability of the equilibrium. For the PDE model, we only have information on the eigenvalues of the generator of the semigroup associated with the linear perturbed system and not the semigroup itself. Compact, eventually compact, and quasi-compact semigroups relate the eigenvalues of the generator to the long-term behavior of the semigroup [40]. The following theorem (Theorem 3.1) suffices to complete the proof of local stability for stationary solutions.

Theorem 3.1. *[40, Theorem B.1] Let $T(t)$ be a quasi-compact C^0- semigroup and A be its infinitesimal generator. Then, $e^{\bar{\delta}t}\|T(t)\| \to 0$ as $t \to \infty$ for some $\bar{\delta} > 0$ if and only if all eigenvalues of A have strictly negative real parts.*

Theorem 3.2. *The disease-free equilibrium is locally asymptotically stable when $\mathcal{R}_0 < 1$ and unstable if $\mathcal{R}_0 > 1$, where,*

$$\mathcal{R}_0 = \frac{r\beta_h}{\mu_1}\int_0^{W_0}\frac{P(W)}{g(W)}e^{-\int_0^W\frac{\mu_2(\tau)}{g(\tau)}d\tau}\,dW + \frac{r\beta_e}{\mu_1}\int_0^{W_0}\frac{\xi(W)}{\sigma}\frac{P(W)}{g(W)}e^{-\int_0^W\frac{\mu_2(\tau)}{g(\tau)}d\tau}\,dW. \tag{3.2}$$

Proof. We let $S(t) = S_0^* + x(t)$, $i(t,W) = i_1(t,W)$, $V = y(t)$ and $B = z(t)$, where $x(t)$, $i_1(t,W)$, $y(t)$ and $z(t)$ are the perturbation variables and S_0^* is the trivial equilibrium point. We substitute these expressions in the system (3.1) and simplify the model by neglecting quadratic perturbation terms that we assume to be much smaller than the perturbations. We, therefore, get the following linearized system:

$$\begin{aligned} \frac{dx(t)}{dt} &= -\mu_1 x(t) - S_0^*\int_0^{W_0}\beta_h P(W) i_1(t,W)\,dW - \beta_e S_0^* z(t) \\ &\quad +\rho y(t) \\ \partial_t i_1(t,W) + \partial_W(g(W)i_1(t,W)) &= -\mu_2(W)i_1(t,W) \end{aligned}$$

$$\begin{aligned} g(0)i_1(t,0) &= S_0^* \int_0^{W_0} \beta_h P(W) i_1(t,W)\, dW + \beta_e S_0^* z(t) \\ \frac{dy(t)}{dt} &= g(W_0) i_1(t,W_0) - \rho y(t) - \mu_3 y(t) \\ \frac{dz(t)}{dt} &= \int_0^{W_0} \xi(W) P(W) i_1(t,W)\, dW - \sigma z(t). \end{aligned} \tag{3.3}$$

Next, we analyse the stability of the linearized system to determine the long-term behavior of the solutions. Since the system is linear, we expect the solutions to be exponential. Thus, we look for solutions of the form $x(t) = \bar{x}e^{\lambda t}$, $i_1(t,W) = \bar{i_1}(W)e^{\lambda t}$, $y(t) = \bar{y}e^{\lambda t}$, $z(t) = \bar{z}e^{\lambda t}$ where $\bar{x}$, $\bar{i_1}(W)$, $\bar{y}$, $\bar{z}$ and λ are to be determined. The λ represents an eigenvalue. Substituting the appropriate formulation in system (3.3) gives us the following eigenvalue problem:

$$\begin{aligned} \lambda\bar{x} &= -\mu_1\bar{x} - S_0^* \int_0^{W_0} \beta_h P(W)\bar{i_1}(W)\, dW - \beta_e S_0^* \bar{z} + \rho\bar{y} \\ \partial_W(g(W)\bar{i_1}(W)) &= -(\mu_2(W) + \lambda)\bar{i_1}(W) \\ g(0)\bar{i_1}(0) &= S_0^* \int_0^{W_0} \beta_h P(W)\bar{i_1}(W)\, dW + \beta_e S_0^* \bar{z} \\ \lambda\bar{y} &= g(W_0)\bar{i_1}(W_0) - \rho\bar{y} - \mu_3\bar{y} \\ \lambda\bar{z} &= \int_0^{W_0} \xi(W) P(W)\bar{i_1}(W)\, dW - \sigma\bar{z}. \end{aligned} \tag{3.4}$$

Now, we are interested in obtaining an equation in terms of λ (characteristic equation). We need to eliminate $\bar{x}$, $\bar{i_1}(W)$, $\bar{y}$, $\bar{z}$ to achieve this. We solve the second equation in system (3.4) to obtain the following:

$$\bar{i_1}(W) = \frac{\bar{i_1}(0)g(0)}{g(W)} e^{-\int_0^W \frac{\mu_2(\tau)+\lambda}{g(\tau)}\, d\tau}.$$

Substituting $\bar{i_1}(W)$ in the the fifth equation of system (3.4) enables us to express $\bar{z}$ as follows:

$$\bar{z} = \frac{\bar{i_1}(0)g(0)}{\lambda + \sigma} \int_0^{W_0} \xi(W) \frac{P(W)}{g(W)} e^{-\int_0^W \frac{\mu_2(\tau)+\lambda}{g(\tau)}\, d\tau}\, dW.$$

We take the expression of $\bar{z}$ and $\bar{i_1}(W)$ and substitute it into the third equation of system (3.4) to obtain the following:

$$\begin{aligned} g(0)\bar{i_1}(0) = S_0^*\bar{i_1}(0)g(0) \Bigg[&\beta_h \int_0^{W_0} \frac{P(W)}{g(W)} e^{-\int_0^W \frac{\mu_2(\tau)+\lambda}{g(\tau)}\, d\tau}\, dW \\ &+ \frac{\beta_e}{\lambda + \sigma} \int_0^{W_0} \xi(W) \frac{P(W)}{g(W)} e^{-\int_0^W \frac{\mu_2(\tau)+\lambda}{g(\tau)}\, d\tau}\, dW \Bigg]. \end{aligned} \tag{3.5}$$

Respectively, we obtain the characteristic equation for λ: $G(\lambda) = 1$ with

$$G(\lambda) = S_0^* \Bigg[\int_0^{W_0} \beta_h \frac{P(W)}{g(W)} e^{-\int_0^W \frac{\mu_2(\tau)+\lambda}{g(\tau)}\, d\tau}\, dW + \frac{\beta_e}{\lambda + \sigma} \int_0^{W_0} \xi(W) \frac{P(W)}{g(W)} e^{-\int_0^W \frac{\mu_2(\tau)+\lambda}{g(\tau)}\, d\tau}\, dW \Bigg]. \tag{3.6}$$

Then, we check the roots of the characteristic equation to deduce the stability. The DFE is stable if the roots of the characteristic equation have negative real parts and it's otherwise unstable.

A non-zero solution to Eq (3.5) exists only if there is a number $\lambda \in \mathbb{R}$ such that $G(\lambda) = 1$. Differentiating equation (3.6) with respect to λ yields $G'(\lambda) < 0$, and thus $G(\lambda)$ is a strictly decreasing function; additionally, $\lim_{\lambda\to\infty} G(\lambda) = 0$. If $\hat{\lambda}$ is a unique real solution of Eq (3.6), then $\hat{\lambda} > 0$, provided $G(0) > 1$ and $\hat{\lambda} < 0$ provided $G(0) < 1$.

We can let $H = S_0^*\beta_h \frac{P(W)}{g(W)} e^{-\int_0^W \frac{\mu_2(\tau)}{g(\tau)}\,d\tau}$ and $J = S_0^*\beta_e \sigma(W) \frac{P(W)}{g(W)} e^{-\int_0^W \frac{\mu_2(\tau)}{g(\tau)}\,d\tau}$ such that,

$$G(\lambda) = \int_0^{W_0} He^{-\int_0^W \frac{\lambda}{g(\tau)}\,d\tau}\,dW + \frac{1}{\lambda+\sigma}\int_0^{W_0} Je^{-\int_0^W \frac{\lambda}{g(\tau)}\,d\tau}\,dW.$$

Suppose $G(0) < 1$ and $\lambda = a \pm bi$ is a complex solution to Eq (3.6) with $a \geq 0$. Then,

$$\begin{aligned} |\, G(\lambda)\,| &= \left|\, \int_0^{\infty} He^{-\int_0^W \frac{\lambda}{g(\tau)}\,d\tau}\,dW + \frac{1}{\lambda+\sigma}\int_0^{\infty} Je^{-\int_0^W \frac{\lambda}{g(\tau)}\,d\tau}\,dW \,\right| \\ &\leq \int_0^{W_0} He^{-\int_0^W \frac{a}{g(\tau)}\,d\tau}\,dW + \frac{1}{(a+\sigma)}\int_0^{W_0} J\, e^{-\int_0^W \frac{a}{g(\tau)}\,d\tau}\,dW = G(a) \leq G(0) < 1. \end{aligned}$$

It follows then that Eq (3.6) has a complex solution $\lambda = a \pm ib$ if $a < 0$, that is, every solution of Eq (3.6) must have a negative real part. We consider $G(0) = 1$ to be the threshold condition for the stability of the disease-free equilibrium. According to [38], this can be defined as the basic reproduction number, that is, $G(0) = \mathcal{R}_0$ where,

$$\mathcal{R}_0 = \frac{r\beta_h}{\mu_1}\int_0^{W_0} \frac{P(W)}{g(W)} e^{-\int_0^W \frac{\mu_2(\tau)}{g(\tau)}\,d\tau}\,dW + \frac{r\beta_e}{\mu_1}\int_0^{W_0} \frac{\xi(W)}{\sigma}\frac{P(W)}{g(W)} e^{-\int_0^W \frac{\mu_2(\tau)}{g(\tau)}\,d\tau}\,dW.$$

By Theorem 3.1, the disease-free equilibrium is locally asymptotically stable.

We can interpret the basic reproduction number to be the total infectivity, given by the following:

$$\mathcal{R}_0 = \mathcal{R}_d + \mathcal{R}_i$$

$$\mathcal{R}_d = \frac{r\beta_h}{\mu_1}\int_0^{W_0} \frac{P(W)}{g(W)} e^{-\int_0^W \frac{\mu_2(\tau)}{g(\tau)}\,d\tau}\,dW, \qquad \mathcal{R}_i = \frac{r\beta_e}{\mu_1}\int_0^{W_0} \frac{\xi(W)}{\sigma}\frac{P(W)}{g(W)} e^{-\int_0^W \frac{\mu_2(\tau)}{g(\tau)}\,d\tau}\,dW.$$

$\mathcal{R}_d$ represents the new infections occurring due to direct contact with an infected individual, while $\mathcal{R}_i$ are the infections resulting from the consumption of contaminated water containing bacteria shed to the environment by infected individuals.

Remark 3.2. *The values in the integral term represent the influence of immunological variables on disease transmission. If within-host dynamics are excluded from the between-host model, the resulting value of $\mathcal{R}_0$ would not account for the role of the immune response in disease dynamics. This implies that disease transmission would primarily depend on other factors, such as the pathogen's transmissibility given by the rates β_e and β_h.*

3.3. Existence of the endemic equilibrium

Proposition 3.3. *A unique positive endemic equilibrium of system (3.1) given by $\mathcal{E}^* = (S^*, i^*(W), V^*, B^*)$ exists if $\mathcal{R}_0 > 1$.*

Proof. The endemic equilibrium satisfies the following equations:

$$\begin{aligned} 0 &= r - \mu_1 S^* - S^* \int_0^{W_0} \beta_h P(W) i^*(W)\, dW - \beta_e S^* B^* + \rho V^* \\ \partial_W(g(W)i^*(W)) &= -\mu_2(W) i^*(W) \\ g(0)i^*(0) &= S^* \int_0^{W_0} \beta_h P(W) i^*(W)\, dW + \beta_e S^* B^* \\ 0 &= g(W_0)i^*(W_0) - \rho V^* - \mu_3 V^* \\ 0 &= \int_0^{W_0} \xi(W) P(W) i^*(W)\, dW - \sigma B^*. \end{aligned} \tag{3.7}$$

Solving the second equation of system (3.7) yields $i^*(W) = \frac{i^*(0)g(0)}{g(W)} e^{-\int_0^W \frac{\mu_2(\tau)}{g(\tau)}\, d\tau}$.

We let $\pi(W) = \frac{1}{g(W)} e^{-\int_0^W \frac{\mu_2(\tau)}{g(\tau)}\, d\tau}$ and rewrite

$$i^*(W) = i^*(0)g(0)\pi(W).$$

Substituting $i^*(W)$ to the fourth and fifth equations of system (3.7) gives the following:

$$B^* = i^*(0)g(0) \int_0^{W_0} \frac{\xi(W)}{\sigma} P(W)\pi(W)\, dW, \qquad V^* = \frac{g(W_0)i^*(0)g(0)\pi(W_0)}{(\rho + \mu_3)}.$$

Plugging $i^*(W)$ and B^* into the boundary equation of system (3.7) yields the following:

$$S^* = \frac{1}{\int_0^{W_0} \beta_h P(W)\pi(W)\, dW + \int_0^{W_0} \beta_e \frac{\xi(W)}{\sigma} P(W)\pi(W)\, dW}.$$

To find the value of $i^*(0)$, we use the first equation of system (3.7), that can be rewritten as the following:

$$r - \mu_1 S^* - g(0)i^*(0) + \rho V^* = 0. \tag{3.8}$$

Notice that S^* can be expressed in terms of $\mathcal{R}_0$, that is, $S^* = \frac{r}{\mu_1 \mathcal{R}_0}$. Substituting S^* and V^* in Eq (3.8) yields the following,

$$r - \frac{r}{\mathcal{R}_0} - g(0)i^*(0) + i^*(0)g(0)\frac{\rho g(W_0)\pi(W_0)}{(\rho + \mu_3)} = 0.$$

Thus, $i^*(0) = \frac{r(1-\frac{1}{\mathcal{R}_0})}{g(0)(1-\frac{\rho g(W_0)\pi(W_0)}{(\rho+\mu_3)})}$. We can then express

$$i^*(W) = \frac{r(1 - \frac{1}{\mathcal{R}_0})}{(1 - \frac{\rho g(W_0)\pi(W_0)}{(\rho+\mu_3)})} \pi(W). \tag{3.9}$$

Since $\frac{\rho g(W_0)\pi(W_0)}{(\rho+\mu_3)} = \frac{\rho e^{-\int_0^W \frac{\mu_2(\tau)}{g(\tau)}\, d\tau}}{(\rho+\mu_3)} < 1$, the denominator in Eq (3.9) is positive. $i^*(W)$ is only positive if $\mathcal{R}_0 > 1$, thus, the endemic equilibrium $\mathcal{E}^* = (S^*, i^*(W), V^*, B^*)$ exists only if $\mathcal{R}_0 > 1$.

3.4. Local stability of the endemic equilibrium

We assume that $\mathcal{R}_0 > 1$ and linearize system (3.1) around the endemic equilibrium. We start by introducing perturbation terms, that is, let $S(t) = S^* + x(t)$, $i(t, W) = i^*(W) + i_1(t, W)$, $V = V^* + y(t)$ and $B = B^* + z(t)$. We substitute these expressions in system (3.1), simplify using the set of equations in system (3.7) and neglect quadratic perturbation terms to get the following linearized system:

$$\begin{aligned}
\frac{dx(t)}{dt} &= -\mu_1 x(t) - S^* \int_0^{W_0} \beta_h P(W) i_1(t, W)\, dW - x(t) \int_0^{W_0} \beta_h P(W) i^*(W)\, d(W) \\
&\quad -\beta_e S^* z(t) - \beta_e B^* x(t) + \rho y(t) \\
\partial_t i_1(t, W) &+ \partial_W (g(W) i_1(t, W)) = -\mu_2(W) i_1(t, W) \\
g(0) i_1(t, 0) &= S^* \int_0^{W_0} \beta_h P(W) i_1(t, W)\, dW + x(t) \int_0^{W_0} \beta_h P(W) i^*(W)\, d(W) \\
&\quad +\beta_e S^* z(t) + \beta_e B^* x(t) \\
\frac{dy(t)}{dt} &= g(W_0) i_1(t, W_0) - \rho y(t) - \mu_3 y(t) \\
\frac{dz(t)}{dt} &= \int_0^{W_0} \xi(W) P(W) i_1(t, W)\, dW - \sigma z(t).
\end{aligned} \tag{3.10}$$

Then, we look for solutions of the form $x(t) = xe^{\lambda t}$, $i_1(t, w) = i_1(W)e^{\lambda t}$, $y(t) = ye^{\lambda t}$, $z(t) = ze^{\lambda t}$. Substituting the appropriate formulation in system (3.10) yields the following eigenvalue problem:

$$\begin{aligned}
\lambda x &= -\mu_1 x - S^* \int_0^{W_0} \beta_h P(W) i_1(W)\, dW - x \int_0^{W_0} \beta_h P(W) i^*(W)\, d(W) \\
&\quad -\beta_e S^* z - \beta_e B^* x + \rho y \\
\partial_W (g(W) i_1(W)) &= -(\mu_2(W) + \lambda) i_1(W) \\
g(0) i_1(0) &= S^* \int_0^{W_0} \beta_h P(W) i_1(W)\, dW + x \int_0^{W_0} \beta_h P(W) i^*(W)\, d(W) \\
&\quad +\beta_e S^* z + \beta_e B^* x \\
\lambda y &= g(W_0) i_1(W_0) - \rho y - \mu_3 y \\
\lambda z &= \int_0^{W_0} \xi(W) P(W) i_1(W)\, dW - \sigma z.
\end{aligned} \tag{3.11}$$

We solve for x, y and z in system (3.11) to get,

$$x = \frac{\rho g(W_0) i_1(W_0) - g(0) i_1(0)(\lambda + \rho + \mu_3)}{(\lambda + \rho + \mu_3)(\lambda + \mu_1)}, \quad y = \frac{g(W_0) i_1(W_0)}{\lambda + \rho + \mu_3},$$
$$z = \frac{1}{\lambda + \sigma} \int_0^{W_0} \xi(W) P(W) i_1(W)\, dW.$$

The solution to the PDE in system (3.11) yields the following:

$$i_1(W) = i_1(0) g(0) \pi_1(W) e^{-\int_0^W \frac{\lambda}{g(\tau)}\, d\tau}, \qquad \pi_1(W) = \frac{1}{g(W)} e^{-\int_0^W \frac{\mu_2(\tau)}{g(\tau)}\, d\tau}.$$

Denoting $K = \int_0^{W_0} \beta_h P(W) i^*(W)\, d(W)$ and substituting x, y, z and $i_1(W)$ in the third equation of system (3.11) gives the following characteristic equation:

$$\begin{aligned} 1 &= S^* \int_0^{W_0} \beta_h P(W)\pi_1(W) e^{-\int_0^W \frac{\lambda}{g(\tau)}\, d\tau}\, dW + \frac{\beta_e S^*}{\lambda+\sigma} \int_0^{W_0} \xi(W) P(W)\pi_1(W) e^{-\int_0^W \frac{\lambda}{g(\tau)}\, d\tau}\, dW \\ &\quad + \frac{(K+\beta_e B^*)(\rho g(W_0)\pi_1(W_0) e^{-\int_0^W \frac{\lambda}{g(\tau)} d\tau})}{(\lambda+\rho+\mu_3)(\lambda+\mu_1)} - \frac{K+\beta_e B^*}{\lambda+\mu_1}. \end{aligned}$$

We can rewrite this equation as the following:

$$\begin{aligned} \frac{\lambda+\mu_1+K+\beta_e B^*}{\lambda+\mu_1} &= S^* \int_0^{W_0} \beta_h P(W)\pi_1(W) e^{-\int_0^W \frac{\lambda}{g(\tau)}\, d\tau}\, dW \\ &\quad + \frac{\beta_e S^*}{\lambda+\sigma} \int_0^{W_0} \xi(W) P(W)\pi_1(W) e^{-\int_0^W \frac{\lambda}{g(\tau)}\, d\tau}\, dW \\ &\quad + \frac{(K+\beta_e B^*)(\rho g(W_0)\pi_1(W_0) e^{-\int_0^W \frac{\lambda}{g(\tau)}\, d\tau})}{(\lambda+\rho+\mu_3)(\lambda+\mu_1)}. \end{aligned} \tag{3.12}$$

Studies have shown that a cholera infection confers immunity against subsequent infection [23]. We consider the case of a single cholera epidemic, where most individuals become immune such that the loss of immunity is negligible. We show that the endemic equilibrium is asymptotically stable.

Theorem 3.3. *Given no loss of immunity* ($\rho = 0$)*, the endemic equilibrium is locally asymptotically stable if* $\mathcal{R}_0 > 1$.

Proof. Considering no loss of immunity, the characteristic equation (3.12) reduces to

$$\begin{aligned} \frac{\lambda+\mu_1+K+\beta_e B^*}{\lambda+\mu_1} &= S^* \int_0^{W_0} \beta_h P(W)\pi_1(W) e^{-\int_0^W \frac{\lambda}{g(\tau)}\, d\tau}\, dW \\ &\quad + \frac{\beta_e S^*}{\lambda+\sigma} \int_0^{W_0} \xi(W) P(W)\pi_1(W) e^{-\int_0^W \frac{\lambda}{g(\tau)}\, d\tau}\, dW. \end{aligned} \tag{3.13}$$

If we let $\lambda = a + ib$ and assume that $a \geq 0$, then for $\mathbb{R}(\lambda) \geq 0$ the left hand side of Eq (3.13) gives,

$$\mid \frac{\lambda+\mu_1+K+\beta_e B^*}{\lambda+\mu_1} \mid = \frac{\sqrt{(a+\mu_1+K+\beta_e B^*)^2+b^2}}{\sqrt{(a+\mu_1)^2+b^2}} > 1,$$

while for $a \geq 0$ the right hand side yields,

$$\begin{aligned} &\mid S^* \int_0^{W_0} \beta_h P(W)\pi_1(W) e^{-\int_0^W \frac{\lambda}{g(\tau)}\, d\tau}\, dW + \frac{\beta_e S^*}{\lambda+\sigma} \int_0^{W_0} \xi(W) P(W)\pi_1(W) e^{-\int_0^W \frac{\lambda}{g(\tau)}\, d\tau}\, dW \mid \\ &\leq S^* \int_0^{W_0} \beta_h P(W)\pi_1(W) \mid e^{-\int_0^W \frac{\lambda}{g(\tau)} d\tau} \mid dW + \frac{\beta_e S^*}{\mid \lambda+\sigma \mid} \int_0^{W_0} \xi(W) P(W)\pi_1(W) \mid e^{-\int_0^W \frac{\lambda}{g(\tau)}\, d\tau} \mid dW \\ &\leq S^* \int_0^{W_0} \beta_h P(W)\pi_1(W) e^{-\int_0^W \frac{a}{g(\tau)}\, d\tau} dW + \frac{\beta_e S^*}{\sigma} \int_0^{W_0} \xi(W) P(W)\pi_1(W) e^{-\int_0^W \frac{a}{g(\tau)}\, d\tau}\, dW \\ &\leq S^* \int_0^{W_0} \beta_h P(W)\pi_1(W)\, dW + \frac{\beta_e S^*}{\sigma} \int_0^{W_0} \xi(W) P(W)\pi_1(W)\, dW = \frac{S^* \mathcal{R}_0 \mu_1}{r} = 1. \end{aligned}$$

Thus, given λ with $\mathbb{R}(\lambda) \geq 0$, the left side of Eq (3.13) is strictly greater than one, while the right side of Eq (3.13) is strictly less than one, which is a contradiction. Therefore, any λ with non-negative real parts can not satisfy the characteristic equation. By Theorem 3.1, the endemic equilibrium is locally asymptotically stable.

4. Discussion

In this paper, we have developed an immuno-epidemiological model to link the within-host and between-host dynamics of cholera. To the best of our knowledge, we have introduced the first attempt to structure the epidemic model of the disease using within-host immune dynamics. We did this by formulating an immunological model that depicted the interaction between the cholera pathogen and the adaptive immune response. We considered a cubic term for pathogen growth to represent Allee effects. Furthermore, the pathogen dynamics were taken to occur on a faster time scale than the immune response dynamics enabling the use of fast-slow methods in the analysis. On the fast time scale, we found stationary solutions and their stability. These results were then used to analyse the reduced problem on a slow time scale. On the slow time scale, we could characterise a single infected individual by their immune response. Then, we scaled up the dynamics of a single infected individual to formulate a structured epidemic model. We established the existence of stationary solutions of the epidemic model and studied their local asymptotic properties by utilizing linearisation techniques and semigroup arguments.

Similar to [16, 17], the within-host model has provided a structure for applying the separation of time-scale methods derived from singular perturbation theory [25, 26] to simplify disease dynamics analysis. Unlike other within-host cholera models, our modeling approach allows for recovery through pathogen clearance after a finite time. In addition, we found minimum pathogen threshold dynamics required for immune response activation. This aligns with experimental studies that show that a critical infectious dose is required for the infection [41]. Our work has also advanced the use of methods for physiologically structured population models [29,32,33,42] in the study of cholera that can be applied to other infectious diseases. In our case, the immune response growth is the velocity vector that describes the change in the physiological variable. The basic reproduction number $\mathcal{R}_0$ of the model was found to represent the contribution of bacteria from the environment (indirect-transmission route) and the human-human (direct transmission) contribution to the infection process, a result that is consistent with single scale models for the disease [13,43]. This suggests that a reduction in reproduction number might be enhanced by intervention strategies targeting pathogen eradication at both human and environmental levels seen in [44, 45]. However, the dependence of $\mathcal{R}_0$ on immunological variables illustrates the difference between the model and the fore-mentioned models. For the DFE, the disease would be eradicated if $\mathcal{R}_0 < 1$ and persist otherwise. A unique endemic equilibrium existed when $\mathcal{R}_0 > 1$ and in the case of no loss of immunity, the endemic equilibrium was locally asymptotically stable.

Although we have provided a novel framework for modelling disease dynamics, our model has several limitations. We have been able to get an appropriate formulation of the I dynamics taking into account the within-host dynamics. However, an appropriate formulation of the influence of population-level interactions in the within-host pathogen load is lacking. For instance, studies have shown that environmental vibrios shape the infectious dose depending on whether they are hyperinfectious or less infectious [11, 12, 23] which in turn can affect within-host pathogen evolution. This contribution of environmental vibrios to the within-host process is neglected in the model. Additionally, the work assumes that one infectious contact is enough to push contacts over the threshold. However, a critical pathogen threshold should be exceeded for the infection to occur, and for subcritical pathogen loads, one infectious contact may not be enough. In our future work, we intend to address these issues.

Use of AI tools declaration

The author declares she has not used Artificial Intelligence (AI) tools in the creation of this article.

Acknowledgments

This research is supported by a grant from the German Academic Exchange Service (DAAD) and by the TUM International Graduate School of Science and Engineering (IGSSE), within the project GENOMIE_QADOP. The author thanks Johannes Müller for his helpful discussions.

Conflict of interest

The author declares there is no conflict of interest.

References

1. W. Garira, A complete categorization of multiscale models of infectious disease systems, *J. Biol. Dyn.*, **11** (2017), 378–435. https://doi.org/10.1080/17513758.2017.1367849
2. H. W. Hethcote, Mathematics of infectious diseases, *SIAM Rev.*, **42** (2000), 599–653. https://doi.org/10.1137/S0036144500371907
3. Z. Feng, J. Velasco-Hernandez, B. Tapia-Santos, M. C. Leite, A model for coupling within-host and between-host dynamics in an infectious disease, *Nonlinear Dyn.*, **68** (2012), 401–411. https://doi.org/10.1007/s11071-011-0291-0
4. Z. Feng, J. Velasco-Hernandez, B. Tapia-Santos, A mathematical model for coupling within-host and between-host dynamics in an environmentally-driven infectious disease, *Math. Biosci.*, **241** (2013), 49–55. https://doi.org/10.1016/j.mbs.2012.09.004
5. Z. Shuai, P. van den Driessche, Global dynamics of cholera models with differential infectivity, *Math. Biosci.*, **234** (2011), 118–126. https://doi.org/10.1016/j.mbs.2011.09.003
6. X. Wang, J. Wang, Modeling the within-host dynamics of cholera: bacterial–viral interaction, *J. Biol. Dyn.*, **11** (2017), 484–501. https://doi.org/10.1080/17513758.2016.1269957
7. M. Martcheva, N. Tuncer, C. St Mary, Coupling within-host and between-host infectious diseases models, *Biomath*, **4** (2015), 1510091. https://doi.org/10.11145/j.biomath.2015.10.091
8. L. M. Childs, F. El Moustaid, Z. Gajewski, S. Kadelka, R. Nikin-Beers, J. W. Smith, et al., Linked within-host and between-host models and data for infectious diseases: a systematic review, *PeerJ*, **7** (2019), e7057. https://doi.org/10.7717/peerj.7057
9. W. Garira, D. Mathebula, R. Netshikweta, A mathematical modelling framework for linked within-host and between-host dynamics for infections with free-living pathogens in the environment, *Math. Biosci.*, **256** (2014), 58–78. https://doi.org/10.1016/j.mbs.2014.08.004
10. M. Ali, A. R. Nelson, A. L. Lopez, D. A. Sack, Updated global burden of cholera in endemic countries, *PLoS Negl. Trop. Dis.*, **9** (2015), e0003832. https://doi.org/10.1371/journal.pntd.0003832
11. D. M. Hartley, J. G. Morris, D. L. Smith, Hyperinfectivity: a critical element in the ability of V. cholerae to cause epidemics, *PLoS Med.*, **3** (2006), e7. https://doi.org/10.1371/journal.pmed.0030007

12. J. Reidl, K. E. Klose, Vibrio cholerae and cholera: out of the water and into the host, *FEMS Microbiol. Rev.*, **26** (2002), 125–139. https://doi.org/10.1016/S0168-6445(02)00091-8

13. Z. Mukandavire, S. Liao, J. Wang, H. Gaff, D. L. Smith, J. G. Morris, Estimating the reproductive numbers for the 2008-2009 cholera outbreaks in Zimbabwe, *PNAS*, **108** (2011), 8767–8772. https://doi.org/10.1073/pnas.1019712108

14. J. P. Tian, J. Wang, Global stability for cholera epidemic models, *Math. Biosci.*, **232** (2011), 31–41. https://doi.org/10.1016/j.mbs.2011.04.001

15. F. Brauer, Z. Shuai, P. van den Driessche, Dynamics of an age-of-infection cholera model, *Math. Biosci. Eng.*, **10** (2013), 1335–1349. https://doi.org/10.3934/mbe.2013.10.1335

16. X. Wang, J. Wang, Disease dynamics in a coupled cholera model linking within-host and between-host interactions, *J. Biol. Dyn.*, **11** (2017), 238–262. https://doi.org/10.1080/17513758.2016.1231850

17. C. Ratchford, J. Wang, Modeling cholera dynamics at multiple scales: environmental evolution, between-host transmission, and within-host interaction, *Math. Biosci. Eng.*, **16** (2019), 782–812 . https://doi.org/10.3934/mbe.2019037

18. J. M. Drake, A. M. Kramer, Allee effects, *Nat. Educ. Knowl.*, **3** (2011), 2.

19. W. C. Allee, Animal aggregations, *Nature*, **128** (1931), 940–941. https://doi.org/10.1038/128940b0

20. R. B. Kaul, A. M. Kramer, F. C. Dobbs, J. M. Drake, Experimental demonstration of an Allee effect in microbial populations, *Biol. Lett.*, **12** (2016), 20160070. https://doi.org/10.1098/rsbl.2016.0070

21. M. Jemielita, N. S. Wingreen, B. L. Bassler, Quorum sensing controls vibrio cholerae multicellular aggregate formation, *eLife*, **7** (2018), e42057. https://doi.org/10.7554/eLife.42057

22. S. Almagro-Moreno, K. Pruss, R. K. Taylor, Intestinal colonization dynamics of Vibrio cholerae, *PLoS Pathog.*, **11** (2015), e1004787. https://doi.org/10.1371/journal.ppat.1004787

23. E. J. Nelson, J. B. Harris, J. G. Morris, S. B. Calderwood, A. Camilli, Cholera transmission: the host, pathogen and bacteriophage dynamic, *Nat. Rev. Microbiol.*, **7** (2009), 693–702. https://doi.org/10.1038/nrmicro2204

24. N. Chaffey, Alberts, B., Johnson, A., Lewis, J., Raff, M., Roberts, K. and Walter, P. Molecular biology of the cell. 4th edn., *Ann. Bot.*, **91** (2003), 401. https://doi.org/10.1093/aob/mcg023

25. C. Kuehn, *Multiple Time Scale Dynamics*, Springer-Verlag, Berlin, 2015. https://doi.org/10.1007/978-3-319-12316-5

26. J. Müller, C. Kuttler, *Methods and Models in Mathematical Biology*, Springer-Verlag, Berlin, 2015. https://doi.org/10.1007/978-3-642-27251-6

27. R. Bertram, J. E. Rubin, Multi-timescale systems and fast-slow analysis, *Math. Biosci.*, **287** (2017), 105–121. https://doi.org/10.1016/j.mbs.2016.07.003

28. J. A. J. Metz, O. Diekmann, *The Dynamics of Physiologically Structured Populations*, Springer-Verlag, Berlin, 1986. https://doi.org/10.1007/978-3-662-13159-6

29. O. Diekmann, M. Gyllenberg, J. Metz, Physiologically structured population models: towards a general mathematical theory, in *Mathematics for Ecology and Environmental Sciences*, Springer-Verlag, Berlin, (2007), 5–20. https://doi.org/10.1007/978-3-540-34428-5_2

30. J. M. Cushing, *An Introduction to Structured Population Dynamics*, SIAM, 1998. https://doi.org/10.1137/1.9781611970005

31. P. Magal, S. Ruan, *Structured Population Models in Biology and Epidemiology*, Springer, 2008. https://doi.org/10.1007/978-3-540-78273-5
32. O. Angulo, F. Milner, L. Sega, A SIR epidemic model structured by immunological variables, *J. Biol. Syst.*, **21** (2013), 1340013. https://doi.org/10.1142/S0218339013400135
33. M. Martcheva, S. S. Pilyugin, An epidemic model structured by host immunity, *J. Biol. Syst.*, **14** (2006), 185–203. https://doi.org/10.1142/S0218339006001787
34. À. Calsina, J. Saldaña, A model of physiologically structured population dynamics with a nonlinear individual growth rate, *J. Math. Biol.*, **33** (1995), 335–364. https://doi.org/10.1007/BF00176377
35. G. F. Webb, *Theory of Nonlinear Age-Dependent Population Dynamics*, CRC Press, 1985.
36. M. Y. Kim, F. A. Milner, A mathematical model of epidemics with screening and variable infectivity, *Math. Comput. Modell.*, **21** (1995), 29–42. https://doi.org/10.1016/0895-7177(95)00029-2
37. N. Kato, H. Torikata, Local existence for a general model of size-dependent population dynamics, *Abstr. Appl. Anal.*, **2** (1997), 207–226. https://doi.org/10.1155/s1085337597000353
38. O. Diekmann, J. A. P. Heesterbeek, J. A. J. Metz, On the definition and the computation of the basic reproduction ratio R0 in models for infectious diseases in heterogeneous populations, *J. Math. Biol.*, **28** (1990), 365–382. https://doi.org/10.1007/BF00178324
39. H. Inaba, *Age-Structured Population Dynamics in Demography and Epidemiology*, Springer, 2017. https://doi.org/10.1007/978-981-10-0188-8
40. M. Martcheva, H. R. Thieme, Progression age enhanced backward bifurcation in an epidemic model with super-infection, *J. Math. Biol.*, **46** (2003), 385–424. https://doi.org/10.1007/s00285-002-0181-7
41. A. N. Gillman, A. Mahmutovic, P. A. zur Wiesch, S. Abel, The infectious dose shapes vibrio cholerae within-host dynamics, *mSystems*, **6** (2021), e0065921. https://doi.org/10.1128/msystems.00659-21
42. M. Gyllenberg, Mathematical aspects of physiologically structured populations: the contributions of J. A. J. Metz, *J. Biol. Dyn.*, **1** (2007), 3–44. https://doi.org/10.1080/17513750601032737
43. J. H. Tien, D. J. D. Earn, Multiple transmission pathways and disease dynamics in a waterborne pathogen model, *Bull. Math. Biol.*, **72** (2010), 1506–1533. https://doi.org/10.1007/s11538-010-9507-6
44. J. Wang, C. Modnak, Modeling cholera dynamics with controls, *Can. Appl. Math. Q.*, **19** (2011), 255–273.
45. R. L. M. Neilan, E. Schaefer, H. Gaff, K. R. Fister, S. Lenhart, Modeling optimal intervention strategies for cholera, *Bull. Math. Biol.*, **72** (2010), 2004–2018. https://doi.org/10.1007/s11538-010-9521-8

AIMS Press